

GREEN BANK TELESCOPE MEASUREMENT OF THE SYSTEMIC VELOCITY OF THE DOUBLE PULSAR BINARY J0737–3039 AND IMPLICATIONS FOR ITS FORMATION

S. M. RANSOM^{1,2}, V. M. KASPI^{1,2,3}, R. RAMACHANDRAN⁴, P. DEMOREST⁴, D. C. BACKER⁴, E. D. PFAHL⁵, F. D. GHIGO⁶,
D. L. KAPLAN⁷

To be submitted to ApJ Letters

ABSTRACT

We report on the measurement at 820- and 1400-MHz of orbital modulation of the diffractive scintillation timescale from pulsar A in the double-pulsar system J0737–3039 using the Green Bank Telescope. Fits to this modulation determine the systemic velocity in the plane of the sky to be $V_{\text{ISS}} \simeq 140.9 \pm 6.2 \text{ km s}^{-1}$. The parallel and perpendicular components of this velocity with respect to the line of nodes of the pulsar’s orbit are $V_{\text{plane}} \simeq 96.0 \pm 3.7 \text{ km s}^{-1}$ and $V_{\text{perp}} \simeq 103.1 \pm 7.7 \text{ km s}^{-1}$ respectively. The large V_{perp} implies that pulsar B was born with a kick speed of $\gtrsim 100 \text{ km s}^{-1}$. Future VLBA determination of the angular proper motion in conjunction with improved V_{ISS} measurements should provide a precise distance to the system. Using high-precision timing data and the V_{ISS} model, we estimate a best-fit orbital inclination of $i = 88.7 \pm 0.9$.

Subject headings: binaries: general — ISM: general — pulsars: general — pulsars: individual (PSR J0737–3039) — stars: kinematics

1. INTRODUCTION

For over twenty years observers have known that measurements of the decorrelation bandwidth $\Delta\nu_d$ and scintillation timescale Δt_d of pulsars undergoing strong Diffractive Interstellar Scintillation (DISS) can be used to estimate their velocity in the plane of the sky (Lyne & Smith 1982). Cordes & Rickett (1998) examined DISS-derived pulsar velocities in detail and found that the measurements depend heavily on the observing frequency, the direction and distance to the pulsar, and the detailed distribution of the interstellar material causing the scintillation. This last point makes measurements of pulsar velocities particularly difficult since different models for the electron distribution and its irregularities can cause differences in the “measured” scintillation velocities (V_{ISS}) by factors of a few. However, for binary pulsars in compact orbits (orbital periods $P_{\text{orb}} \lesssim 1$ day), the pulsar-timing-derived orbital velocities can be used to calibrate V_{ISS} measurements and remove many model-dependent and/or systematic effects. Unfortunately, suitable binary pulsars are rare and successful measurements of this kind have only been made for two pulsars: PSR B0655+64 by Lyne (1984) and PSR J1141–6545 by Ord, Bailes, & van Straten (2002, hereafter OBVS).

PSRs J0737–3039A & B (hereafter A and B; Burgay et al. 2003; Lyne et al. 2004) comprise a fantastic double-pulsar binary (hereafter 0737) consisting of the 22.7-ms pulsar A and the 2.77-s pulsar B. It is nearby (~ 0.6 kpc), mildly eccentric ($e \sim 0.088$), compact ($P_{\text{orb}} \sim 2.45$ h), highly inclined

($i \sim 87^\circ$), strongly relativistic, and displays eclipses of A and very large but systematic flux variations of B. Its proximity, relatively high measured flux density, and rapidly moving pulsars (orbital velocities $\sim 300 \text{ km s}^{-1}$), make it an ideal target for V_{ISS} studies. In this paper we report measurements of the orbital modulation of V_{ISS} from A at 820- and 1400-MHz using data from the 100-m Green Bank Telescope (GBT).

2. OBSERVATIONS AND DATA REDUCTION

In 2003 December, our group was awarded 5×6 hr Exploratory Time tracks on 0737 with the GBT as part of the NRAO Rapid Science program. Three of the observations discussed in this paper were made with the Berkeley-Caltech Pulsar Machine (BCPM; e.g. Kaspi et al. 2004) using summed IFs and $72 \mu\text{s}$ sampling; one at 1400 MHz using 96×1 MHz channels and the other two at 820 MHz using 96×0.5 MHz channels (Table 1). During one 820 MHz observation, we also obtained data with the GBT Spectrometer SPIGOT Card, a new, flexible, and high performance pulsar backend developed at Caltech and NRAO. It processes auto-correlations from the GBT Digital Spectrometer using two custom digital logic cards. These cards accumulate, sort, pack, and decimate the data before sending it to a PC for further packing and output into FITS files on a multi-TB RAID array. The SPIGOT currently handles one or two IFs with bandwidths of 50- or 800-MHz. We used a 50 MHz mode (#44) to process 1024 lags from summed IFs that were 8-bit sampled every $40.96 \mu\text{s}$. In total, the SPIGOT observation generated 420 GB of data which we recorded onto removable hard disks.

We folded these data modulo the predicted pulse period given the timing solution from Lyne et al. (2004). These folds were used to determine a local timing solution for A and to create dynamic spectra from which to measure scintillation parameters. For the timing analysis, we measured 300 times-of-arrival (TOAs) from each of the observations (for individual integration times of ~ 1 min) by cross-correlating the folded profiles with a template profile from the SPIGOT data and then referencing the maximum of the cross-correlation with the time of the start of the observation as determined from the observatory clock. Our initial timing

¹ Department of Physics, Rutherford Physics Building, McGill University, 3600 University Street, Montreal, Quebec, H3A 2T8, Canada; ransom@physics.mcgill.ca

² Department of Physics and Center for Space Research, Massachusetts Institute of Technology, Cambridge, MA 02139

³ Canada Research Chair; NSERC Steacie Fellow

⁴ Department of Astronomy, University of California, 601 Campbell Hall, Berkeley, CA 94720

⁵ Chandra Fellow; Harvard-Smithsonian Center for Astrophysics, 60 Garden Street, Cambridge, MA 02138

⁶ National Radio Astronomy Observatory, P.O. Box 2, Green Bank, WV 24944

⁷ Department of Astronomy, California Institute of Technology, MS 105-24, Pasadena, CA 91125

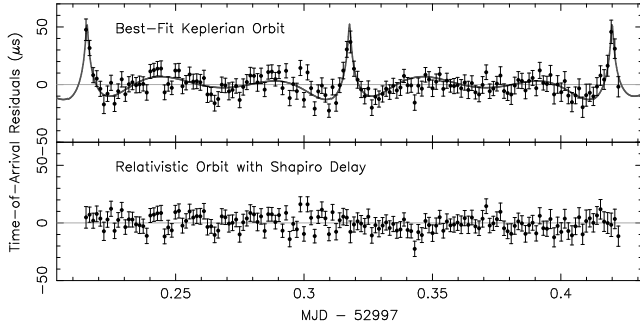


FIG. 1.— Timing results from the 820 MHz GBT+SPIGOT observation listed in Table 1. (Top) Residuals from a Keplerian orbit fit to the data. Systematic deviations corresponding to the unmodeled Shapiro delay (shown as the line) are obvious in each orbit. (Bottom) Residuals from a fit using the “DD” timing model which includes the Shapiro delay for a $1.25 M_{\odot}$ pulsar B at an orbital inclination $i=88.4^{\circ}$. The post-fit RMS residuals for the SPIGOT data alone are $<7 \mu\text{s}$.

fits using TEMPO⁸ showed approximately linear, frequency-dependent drifts in the TOAs of tens of μs during each of the 5–6 hr observations. Since A’s pulsations are significantly linearly polarized (Demorest et al. 2004), such apparent drifts may be caused by changes in the total-intensity pulse profile with time due to the rotation of the receiver feed with respect to the sky and gain differences in the two orthogonal IFs that were summed. In order to make high-precision measurements of *local* effects like the Shapiro delay, we fit for frequency jumps between the observations which effectively whitened the residuals to provide a post-fit RMS of $\sim 11 \mu\text{s}$. Using a mass for B of $1.25 M_{\odot}$ (Lyne et al. 2004), we determine the Shapiro “shape” parameter to be $\sin i = 0.99962^{+0.00038}_{-0.00095}$ which corresponds to an inclination of $88.4^{+1.6}_{-1.4}$. The errors for $\sin i$ and the other orbital parameters were determined using a bootstrap analysis (e.g. Efron & Tibshirani 1986) which showed that our results are consistent with those in Lyne et al. (2004) at the $1\text{-}\sigma$ level. Figure 1 shows residuals from the 820 MHz GBT+SPIGOT observation alone.

Assuming a uniform Kolmogorov scattering medium, Cordes & Rickett (1998) derived the velocity estimator

$$V_{\text{ISS}} = 2.53 \times 10^4 \frac{\sqrt{D \Delta\nu_d}}{\nu \Delta t_d} \text{ km s}^{-1}, \quad (1)$$

where D is the distance to the source in kpc, $\Delta\nu_d$ is the decorrelation bandwidth in MHz, Δt_d is the scintillation timescale in seconds, and ν is the observing frequency in GHz. Note that unlike Δt_d , which varies based on the relative velocities of the Earth, scintillation screen, and pulsar, $\Delta\nu_d$ is a property of the screen itself and therefore does not vary significantly during an observation. The initial constant differs by factors of $\sim 1\text{--}3$ depending on the structure function of the scattering medium/screen as well as its location and extent. The key point is that $V_{\text{ISS}} \propto \Delta t_d^{-1}$, with an overall scaling that can be *measured* by fitting the known orbital velocity of the pulsar to the measured changes in Δt_d .

In order to determine Δt_d and $\Delta\nu_d$ for each of the observations listed in Table 1, we closely followed the process described in OBvS. Briefly, we created calibrated dynamic spectra (see fig. 2) by taking the on-pulse minus off-pulse flux during a duration T_{int} divided by the average level in each frequency channel during the full observation. We then computed the autocorrelation function (ACF) of non-overlapping

(and hence independent) blocks of the dynamic spectra of duration T_{meas} in order to measure Δt_d (defined as the $1/e$ half-width of the central ACF peak in the time direction; Cordes 1986). We measured $\Delta\nu_d$ (defined as the half-width at half-height of the central ACF peak in the frequency direction; Cordes 1986) and its errors by fitting gaussians to the central ACF peaks from 15 sub-integrations and examining their statistics. We determined the relative errors for the Δt_d values similarly, by examining the statistics for Δt_d fits made in 6 and 3 frequency subbands for the SPIGOT and BCPM data respectively. Due to the small number of available subbands, we added additional errors of 5 and 10 km/s in quadrature to the measured errors for the SPIGOT and BCPM data respectively to guard against underestimates of V_{ISS} errors.

We converted the measured Δt_d values into uncalibrated V_{ISS} measurements using eq. 1, and calculated the true anomaly Θ at the center of each V_{ISS} measurement interval using the timing ephemeris from Lyne et al. (2004). We performed a weighted least-squares fit of these data to eq. 7 in OBvS, $V_{\text{ISS}} = \kappa(\nu'^2 + \nu''^2)^{1/2}$, where ν' and ν'' are the total velocities (i.e. orbital + systemic) parallel to and perpendicular to the orbital line of nodes in the plane of the sky respectively. In contrast to OBvS, we used the angle of periastron ω from the timing ephemeris and fit for four parameters; the systemic velocities parallel to (V_{plane}) and perpendicular to (V_{perp}) the line of nodes, the inclination i , and the scaling parameter κ . Fitting for κ accounts for uncertainties in the nature of the scattering medium and the distance to the pulsar. Table 1 lists the fitted parameters and their 95% statistical confidence limits as determined from projections of the χ^2 space. The knowledge that we observe 0737 nearly edge-on ($i \sim 90^{\circ}$) removes the degeneracy in possible inclination angles seen by Lyne (1984) and OBvS and produces a single solution for each observation. The errors in the fitted parameters were calculated after scaling the Δt_d errors such that the reduced- χ^2 of the fits equaled one. Combining the BCPM and SPIGOT results provides our best estimates of $V_{\text{plane}} \simeq 96.0 \pm 3.7 \text{ km s}^{-1}$ and $V_{\text{perp}} \simeq 103.1 \pm 7.7 \text{ km s}^{-1}$ for a total systemic velocity in the plane of the sky of $V_{\text{ISS}} \simeq 140.9 \pm 6.2 \text{ km s}^{-1}$.

We note that V_{ISS} fits can result in $i > 90^{\circ}$. In that case (as we have measured), the direction of V_{perp} is either aligned with the orbital angular momentum vector if it is pointing slightly towards us, or anti-aligned if the angular momentum is pointing slightly away from us. Combining the timing- and scintillation-based measurements gives an inclination (in the more standard range $0^{\circ}\text{--}90^{\circ}$) of $i = 88.7 \pm 0.9$.

2.1. Possible Biases to the Measured V_{ISS}

While the “self-calibrating” nature of binary pulsar V_{ISS} measurements eliminates many of the uncertainties found in V_{ISS} studies of isolated pulsars (e.g. Cordes 1986), the motion of the Earth with respect to the pulsar and the differential rotation of the Galaxy both contribute to the measured V_{ISS} .

A flat, 220 km s^{-1} , Galactic rotation curve implies a velocity component in the plane of the sky of $\Delta V_{g\perp} \simeq 14(D/0.6 \text{ kpc}) \text{ km s}^{-1}$ due to differential Galactic rotation in the direction of 0737 ($l = 245.2^{\circ}$, $b = -4.5^{\circ}$). However, as Cordes & Rickett (1998) point out, the ISM rotates along with the Galaxy, and we calculate that the *effective* transverse velocity is $< 1 \text{ km s}^{-1}$ for all reasonable distances to 0737.

Earth’s orbital motion projected onto the sky towards 0737 contributes a doubly periodic velocity component $\Delta V_{\oplus\perp}$ to the measured V_{ISS} . For 0737, $\Delta V_{\oplus\perp}$ has minimum and max-

⁸ <http://pulsar.princeton.edu/tempo>

TABLE 1
GBT OBSERVATIONS AND V_{ISS} MODEL FITS FOR J0737–3039A

f_{ctr} (MHz)	Start MJD	Freq. Res. (bands \times MHz)	T_{obs} (hr)	T_{int} (s)	T_{meas} (s)	$\Delta\nu_d$ (MHz)	V_{ISS} (km/s)	V_{plane} (km/s)	V_{perp} (km/s)	i (deg)	κ	χ^2/DOF
820 ^a	52997.214	1024 \times 0.04883	5.00	10.0	320	0.096(4)	139.0(4.5)	95.1(3.8)	101.4(8.0)	91.0(1.1)	0.631(11)	0.64
1400 ^b	52984.195	96 \times 1.0	6.12	12.24	612	1.8(2)	163(16)	107(13)	123(27)	92.9(3.5)	0.693(48)	1.50

NOTE. — ^a SPIGOT data. ^b BCPM data. All confidence intervals are 95% statistical. The number of degrees of freedom for the model fits are $\text{DOF}_{820} = 56 - 4 = 52$ and $\text{DOF}_{1400} = 36 - 4 = 32$. For these measurements, i can range from 0–180° (see §2). The errors on the fitted parameters were determined from projections of the χ^2 space after adjusting the errors of the V_{ISS} measurements such that $\chi^2/\text{DOF}=1$.

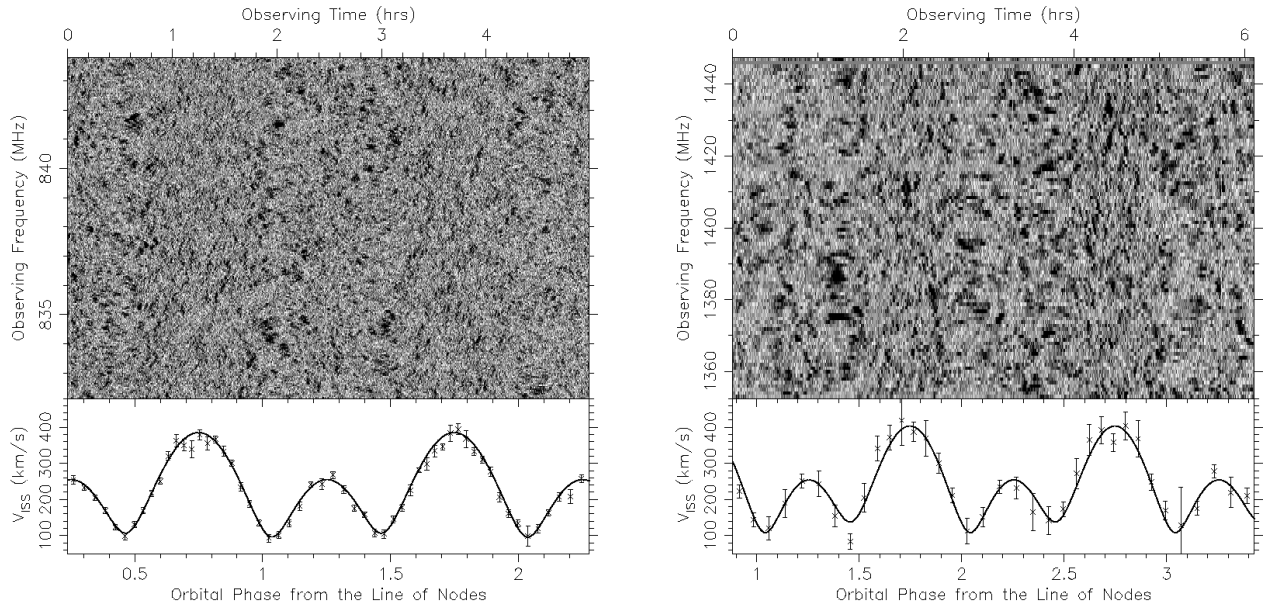


FIG. 2.— Dynamic spectra (top) and V_{ISS} model fits (bottom) for the observations listed in Table 1. The 820 MHz SPIGOT data is on the left and the 1400 MHz BCPM data is on the right. For the SPIGOT dynamic spectra, only the top 1/4 of the analyzed band is plotted. Values $\pm 2\sigma$ from the average level were set to black/white respectively in order to enhance the contrast.

imum values of 23 and 30 km s^{-1} respectively. During these observations, $\Delta V_{\oplus\perp} \sim 29 \text{ km s}^{-1}$.

Since we do not know the orientation of the measured V_{ISS} on the plane of the sky, we cannot currently remove either of these biases from our data. However, measurement of an annual variation in V_{ISS} would allow us to remove $\Delta V_{\oplus\perp}$. Alternatively, VLBA determination of the proper motion direction will allow us to subtract both biases directly. In addition, the combination of the VLBA angular proper motion μ with the transverse velocity $V_{\perp} \simeq V_{\text{ISS}}$ will provide a unique geometric distance to the pulsar ($D = V_{\perp}/\mu$).

3. DISCUSSION

The relatively large $V_{\text{ISS}} \simeq 140 \text{ km s}^{-1}$ measured for 0737 has important implications for the formation of the system. Here we assume that 0737 followed the standard formation scenario for double neutron stars (DNSs) in the Galactic disk (e.g. Bhattacharya & van den Heuvel 1991). In this picture, the first NS (A) forms in orbit about a massive ($\gtrsim 8 M_{\odot}$) stellar companion. The binary acquires some velocity due to impulsive mass loss in the supernova explosion and a possible natal kick to the NS. At this stage, the system resembles a high-mass X-ray binary (HMXB). Detailed studies (e.g., Pfahl et al. 2002) find expected HMXB systemic speeds $\lesssim 30 \text{ km s}^{-1}$, because the NS kick is distributed over the large

total mass of the binary. It is unlikely that the first supernova provided the high systemic velocity implied by the measured V_{ISS} .

At the end of the HMXB phase of DNS formation, the stellar companion evolves, fills its Roche lobe, and transfers matter to the NS. Because of the extreme mass ratio of the binary, the transfer is dynamically unstable, and leads to a common-envelope phase. If coalescence is avoided, the NS emerges in a tight orbit with the hydrogen-exhausted core of its companion. The stellar core continues its nuclear evolution, and may stably transfer matter to the NS via Roche-lobe overflow. This is the favored mechanism for spinning up and reducing the dipole magnetic field strength of A (Dewi & van den Heuvel 2004). Subsequently, the stellar core explodes and produces the second NS (B). In 0737, the pre-supernova mass of the stellar core was likely $M_c \simeq 2.0\text{--}3.5 M_{\odot}$ (Dewi & van den Heuvel 2004; Willems & Kalogera 2004). The combination of supernova mass loss and a kick to B could easily have given 0737 a speed of $\gtrsim 140 \text{ km s}^{-1}$. We now use the interestingly large component ($V_{\text{perp}} \simeq 103 \text{ km s}^{-1}$) of the systemic velocity perpendicular to the orbital plane to constrain the magnitude of the kick imparted to B.

The masses of A and B are $M_A \simeq 1.34 M_{\odot}$ and $M_B \simeq 1.25 M_{\odot}$ respectively, giving a total binary mass of $M_t =$

$M_A + M_B \simeq 2.59 M_\odot$ (Lyne et al. 2004). We assume that the pre-supernova orbit was circular, and denote by \mathbf{R} , \mathbf{V} , and $\mathbf{H} = \mathbf{R} \times \mathbf{V}$ the position, velocity, and orbital angular momentum of the pre-collapse progenitor of B relative to A. If B receives an impulsive natal kick velocity of \mathbf{V}_k , the post-supernova relative orbital velocity and angular momentum are given, respectively, by $\mathbf{V}' = \mathbf{V} + \mathbf{V}_k$ and $\mathbf{H}' = \mathbf{H} + \mathbf{R} \times \mathbf{V}_k$. The velocity acquired by the binary center of mass after the supernova is

$$\mathbf{V}_{\text{CM}} = -\frac{M_A (M_c - M_B)}{M_t (M_c + M_A)} \mathbf{V} + \frac{M_B}{M_t} \mathbf{V}_k. \quad (2)$$

If $\mathbf{V}_k = 0$, then \mathbf{V}_{CM} is in the orbital plane. Therefore, the large observed perpendicular component of V_{ISS} , V_{perp} , may require B to have been born with a significant kick velocity. If we assume that \mathbf{V}_{CM} , and thus the observed V_{perp} , is entirely due to the second supernova explosion, it is straightforward to show that V_{perp} is related to \mathbf{V}_k by (see also Wex et al. 2000)

$$\mathbf{H}' \cdot \mathbf{V}_{\text{CM}} = H' V_{\text{perp}} = \mathbf{H} \cdot \mathbf{V}_k \left(1 + \frac{M_A}{M_c}\right)^{-1}. \quad (3)$$

For specified masses and orbital parameters before and after the supernova, V_k is minimized when \mathbf{V}_k is parallel to \mathbf{H} (i.e., perpendicular to the pre-supernova orbital plane). The minimum kick speed is then

$$V_{k,\text{min}} = V_{\text{perp}} \frac{H'}{H} \left(1 + \frac{M_A}{M_c}\right). \quad (4)$$

Note that

$$\frac{H'}{H} = \left[\left(\frac{M_t}{M_c + M_A} \right) \frac{a'}{a} (1 - e'^2) \right]^{1/2}, \quad (5)$$

where a' and e' are the immediate post-supernova semi-major axis and eccentricity, respectively, which have since evolved to their observed values under the action of gravitational wave emission. Dewi & van den Heuvel (2004) and Willems & Kalogera (2004) each find that $e' \lesssim 0.14$, so that a'/a cannot differ substantially from unity. For our purposes, it is sufficient to assume that $(a'/a)(1 - e'^2) \simeq 1$. Finally, we obtain

$$V_{k,\text{min}} \simeq V_{\text{perp}} \left(\frac{M_t}{M_c} \right)^{1/2} \left(1 + \frac{M_A}{M_c} \right)^{1/2}. \quad (6)$$

For the range of pre-collapse core masses given above, and $V_{\text{perp}} \simeq 100 \text{ km s}^{-1}$, we find that $V_{k,\text{min}} \simeq 100\text{--}150 \text{ km s}^{-1}$, where the upper limit corresponds to $M_c = 2M_\odot$. If the pre-supernova core mass takes its smallest possible value of $M_c = M_B$, then $V_{k,\text{min}} \simeq 213 \text{ km s}^{-1}$.

Piran & Shaviv (2004) point out that at a distance of 0.6 kpc, 0737 is only $\sim 50 \text{ pc}$ from the Galactic plane. They suggest that in order to find 0737 so close to the plane, \mathbf{V}_{CM} must be very small ($\lesssim 15 \text{ km s}^{-1}$ or $\lesssim 150 \text{ km s}^{-1}$ at 68% or 95% confidence respectively), and that the supernova mass loss and

kick to B must likewise have been very small. The measurement of a large V_{ISS} implies that (1) either the velocity direction is largely in the Galactic plane or we happen to see it as it passes through the plane, and (2) moderate pre-collapse core masses and NS kicks are permitted if not required.

VLBA observations will soon determine the magnitude and direction of 0737's proper motion $\mu \simeq 0.05'' \text{ yr}^{-1} (V_{\text{ISS}}/140 \text{ km s}^{-1})(D/0.6 \text{ kpc})^{-1}$. For long-term timing observations, the large velocity in the plane of the sky $V_\perp \simeq V_{\text{ISS}}$ will cause an apparent acceleration (Shklovskii 1970) that will bias the measured spin- and orbital-period derivatives. For 0737, $\dot{P}/P = V_\perp^2/(Dc) = V_\perp \mu/c \simeq 3.5 \times 10^{-18} \text{ s}^{-1}$, which amounts to $\sim 5\%$ of A's measured spindown and $\sim 2.5\%$ of the predicted orbital decay rate due to gravitational wave emission. Future bias-corrected measurements of V_{ISS} should determine V_\perp to a few percent and VLBA observations will likely measure μ to even better precision. Therefore, the ‘‘Shklovskii effect’’ should be measurable to $\lesssim 5\%$ precision and consequently, its error will contaminate the measurement of the orbital period-derivative \dot{P}_{orb} due to the emission of gravitational wave emission by $\lesssim 0.2\%$.

4. CONCLUSIONS

We have measured the systemic velocity and inclination of 0737 using the ‘‘self-calibrating’’ method of binary scintillation velocity measurements. The inferred high velocity $V_{\text{ISS}} \simeq 140 \text{ km s}^{-1}$ strongly suggests that a substantial ($\gtrsim 100 \text{ km s}^{-1}$) kick was imparted to pulsar B at its birth. The large V_{ISS} will impact long-term timing of the system and will allow a precise geometric distance measurement when combined with a VLBA proper motion.

Future scintillation observations using the high frequency resolution and wide bandwidth of the GBT+SPIGOT will allow substantially improved measurements of V_{ISS} at 1400 and even 2200 MHz where we have already detected the orbital modulation of A in BCPM data. These measurements should also allow the removal of the contaminating effects of the Earth's motion and the differential Galactic rotation. Finally, we have already detected scintillation from B during the bright portions of its orbit, but future observations may allow ‘‘snapshot’’ calibrations of V_{ISS} based on measurements of Δt_d from A and B at an instant in time given our knowledge of the relative orbital velocities of the pulsars. Such measurements would demand far less telescope time.

Acknowledgements We extend special thanks to Karen O'Neil, Rich Lacasse, Glen Langston, and Chris Clark for help with the observations. The National Radio Astronomy Observatory is a facility of the National Science Foundation operated under cooperative agreement by Associated Universities, Inc. V.M.K. acknowledges support from NSERC Discovery Grant 228738-03, NSERC Steacie Supplement 268264-03, a Canada Foundation for Innovation New Opportunities Grant, FQRNT Team and Centre Grants, and NASA Long-Term Space Astrophysics Grant NAG5-8063.

REFERENCES

- Bhattacharya, D. & van den Heuvel, E. P. J. 1991, *Phys. Rep.*, 203, 1
 Burgay, M., D'Amico, N., Possenti, A., Manchester, R. N., Lyne, A. G., Joshi, B. C., McLaughlin, M. A., Kramer, M., Sarkissian, J. M., Camilo, F., Kalogera, V., Kim, C., & Lorimer, D. R. 2003, *Nature*, 426, 531
 Cordes, J. M. 1986, *ApJ*, 311, 183
 Cordes, J. M. & Rickett, B. J. 1998, *ApJ*, 507, 846
 Demorest, P., Ramachandran, R., Backer, D. C., Ransom, S. M., Kaspi, V. M., Arons, J., & Spitkovsky, A. 2004, *ApJ*, submitted (astro-ph/0402025)
 Dewi, J. D. M. & van den Heuvel, E. P. J. 2004, *MNRAS*, 349, 169
 Efron, B. & Tibshirani, R. 1986, *Stat. Sci.*, 1, 54
 Kaspi, V. M., Ransom, S. M., Backer, D. C., Ramachandran, R., Demorest, P., Arons, J., & Spitkovsky, A. 2004, *ApJ*, submitted (astro-ph/0401614)
 Lyne, A. G. 1984, *Nature*, 310, 300

- Lyne, A. G., Burgay, M., Kramer, M., Possenti, A., Manchester, R. N., Camilo, F., McLaughlin, M. A., Lorimer, D. R., D'Amico, N., Joshi, B. C., Reynolds, J., & Freire, P. C. C. 2004, *Science*, 303, 1153
- Lyne, A. G. & Smith, F. G. 1982, *Nature*, 298, 825
- Ord, S. M., Bailes, M., & van Straten, W. 2002, *ApJ*, 574, L75
- Pfahl, E., Rappaport, S., Podsiadlowski, P., & Spruit, H. 2002, *ApJ*, 574, 364
- Piran, T. & Shaviv, N. J. 2004, *ArXiv Astrophysics e-prints*, (astro-ph/0401553)
- Shklovskii, I. S. 1970, *Soviet Ast.*, 13, 562
- Wex, N., Kalogera, V., & Kramer, M. 2000, *ApJ*, 528, 401
- Willems, B. & Kalogera, V. 2004, *ApJ*, 603, L101